

Initial stages of cesium incorporation on keV-Cs⁺-irradiated surfaces: Positive-ion emission and work-function changes

Hubert Gnaser

Fachbereich Physik and Institut für Oberflächen- und Schichtanalytik, Universität Kaiserslautern, D-67663 Kaiserslautern, Germany

(Received 6 May 1996; revised manuscript received 15 July 1996)

The gradual incorporation of cesium into elemental samples of Al, Si, Nb, and Au bombarded with 5.5-keV Cs⁺ ions was investigated by monitoring the emission of sputtered positive Cs⁺ and molecular ions and the relative work-function changes ($\Delta\Phi$) induced from the shifts of secondary-ion energy distributions. With increasing Cs fluence and Cs surface concentration the work function is reduced, and reaches a stationary value at about 1×10^{16} Cs⁺/cm² for Si and Al, 5×10^{15} Cs⁺/cm² for Nb, and 1.5×10^{15} Cs⁺/cm² for Au. The corresponding $\Delta\Phi$ shifts then amount to -1.3 ± 0.1 eV for Al and Si, -0.9 eV for Nb, and -0.4 eV for Au. This lowering of the work function reduces the ionization probability of positive Cs⁺ ions by factors of about ten (Al), seven (Si), and three (Nb). In agreement with the electron-tunneling model of secondary-ion formation, this reduced ionization is observed only when the work function falls below a limiting value which is close to the ionization potential of Cs. Computer simulations of the Cs incorporation process result in stationary Cs surface concentrations of 12 at. % for Si, 10% for Al, 5.5% for Nb, and $\sim 2.5\%$ for Au. These values scale inversely with these elements' sputtering yields. [S0163-1829(96)00447-X]

INTRODUCTION

It was realized a long time ago¹ that sputtered negative-ion emission is strongly enhanced by the presence of alkali metals at the ions' emission site on the surface. This finding is widely utilized² in secondary-ion-mass spectrometry (SIMS) for the sensitive detection of electronegative elements by monitoring their respective negatively charged secondary ions. Most often, this enhancement is accomplished by employing a Cs⁺ primary ion beam for sputtering, thus loading the near-surface region of the bombarded specimen with cesium. In general, the resulting amount of Cs at the surface is not known, but can be expected to depend on a variety of parameters like the projectile's energy and incidence angle, the specimen's sputtering yield and, possibly, others.^{3,4} The increase of the ionization probability of sputtered negative secondary ions in the presence of Cs has been ascribed to a lowering of the sample's work function (WF) (in fact, its surface contribution is lowered due to the development of a surface dipole layer, with the positive charge of Cs⁺ farther away, and an electron donated to the substrate). An exponential dependence on the work function Φ is predicted by several theoretical approaches, and was verified by static alkali-metal adsorption experiments (for a comprehensive review, see Ref. 5). Generally, in these investigations the amount of alkali-metal atoms is well controlled and can be derived from, e.g., Auger-electron-spectroscopy data. By contrast, for the *dynamic* SIMS conditions described above (Cs⁺ is used as the bombarding species), existing results on the Cs-surface concentration are rather conflicting,^{4,6} while essentially nothing is known about the WF changes associated with this Cs incorporation.

The presence of alkali atoms (in particular Cs) on the surface also strongly influences the emission of positive ions.⁷ Although perhaps less clearcut, a dependence on the WF is again observed; however, the direction of variation is

reversed for positive ions: a *lowering* of the work function *reduces* the probability to form a *positive* secondary ion. While for usual SIMS analyses this effect is of little concern (oxygen primary beams are commonly used for positive-ion detection), it does apparently influence the emission of so-called *MCs⁺* molecular ions (*M* stands for an atom of the sample material). These species are (abundantly) formed under Cs⁺ bombardment (i.e., from Cs-loaded surfaces) from essentially all elements.² Their analytical usefulness lies in the observation that matrix effects (that is, drastic variations of ions yields with sample composition), which are common for atomic ions, appear⁸ to be largely absent for *MCs⁺*. This was rationalized by their possible formation mechanism: the association of a *neutral M* atom with a Cs⁺ ion in the sputtering event. Clearly, for such a process the amount of sputtered Cs⁺ is of utmost importance, as it should determine the number of actually formed *MCs⁺* ions. Since little information is available as to the equilibrium Cs concentration building up at the surface upon dynamic Cs⁺ bombardment (and the WF changes induced thereby), predictions on the Cs⁺ yield and its variations in different substrates (e.g., in a depth-profile analysis) are virtually impossible.

Theoretical descriptions of secondary-ion emission (like the electron-tunneling mode⁷ and others⁵) predict an exponential dependence of the ionization probability of positive ions, P^+ , on the WF, and the atom's ionization potential I :

$$P^+ \propto \exp[-(I - \Phi)/\epsilon_0]. \quad (1)$$

The parameter ϵ_0 is considered to scale with the normal component of the ion's emission velocity. While some experiments^{9,10} appear to confirm this prediction, others¹¹ find ϵ_0 to be (almost) independent of velocity. Also, the former data tend to exhibit a leveling off (toward a constant value) for low velocities. Furthermore, a velocity dependence in Eq. (1) should become manifest in *pronounced* differences of the secondary ions' energy distributions with

small changes of $(I-\Phi)$.¹² It is commonly assumed that energy spectra of sputtered ions can be factorized into the distribution of the neutral species and the ionization term as given by Eq. (1). The former is known¹³ to exhibit a dependence on the emission energy E proportional to $E/(E+U)^3$, where U is the surface binding energy the departing atoms have to surmount. This scaling produces the peak of the distribution to occur at $U/2$, i.e., at a few eV for most materials. With a velocity-dependent term in Eq. (1), for sputtered ions this peak should move to higher energies. This shift would increase with increasing $(I-\Phi)$. For example,¹⁴ Ga^+ and As^+ sputtered from GaAs have P^+ values differing by about three orders of magnitude, since $I_{\text{Ga}}=6.0$ eV and $I_{\text{As}}=9.8$ eV, but their energy spectra are very similar with respect to the peak position. Equation (1), on the other hand, would predict a difference of some 10 eV or more.¹² The same argument should also hold for changes of Φ . The present experiments indicate, however, that the shape of the energy spectra does not change (at least in the low-energy portion) with moderate Φ variations (see below).

Very important in this context is the experimental finding (and the associated theoretical description) that the ionization probability is unity for $\Phi>I$.⁷ Since $I_{\text{Cs}}=3.89$ eV, one may expect $P_{\text{Cs}}^+=1$ for most clean surfaces, with *no* dependence on emission velocity. Only a lowering of the WF due to Cs incorporation might reduce P_{Cs}^+ . Conversely, if this reduction is not sufficient to reach $I>\Phi$ (due to, e.g., too low a stationary Cs concentration), P_{Cs}^+ should remain unity. The present data will illustrate both of these possibilities.

This work aimed to determine *in situ*, under dynamic Cs^+ irradiation conditions, transient work-function changes as well as the variation of Cs^+ (and MCs^+) yields. To this end, pristine surfaces of elemental samples were exposed to the Cs^+ primary-ion beam (impact energy 5.5-keV) in an incremental fashion by recording repeatedly energy distributions of Cs^+ and MCs^+ ions. Their energy shifting is indicative of a variation of the contact potential between the sample (and thus of the variation of the WF) and the energy analyzer. WF changes of about 0.1 eV are detectable by these means (see below). Clearly, this kind of a WF determination should be sensitive to the aforementioned possible changes of energy spectra. It will be shown that these are largely absent for the present experimental situation. It is noted that this onset method of a (relative) WF determination is often employed using secondary electrons,^{15,16} but has also been utilized in static Cs adsorption experiments.^{11,17} The present work, however, appears to constitute the first application to dynamic Cs implantation conditions which are relevant for common SIMS analyses. Furthermore, it attempts to correlate Cs^+ and MCs^+ ion yields during the gradual cesium buildup at the surface.

EXPERIMENT

The experiments were performed in a secondary-ion microscope [Cameca IMS 4f (Ref. 18)]. This instrument has a double-focusing mass spectrometer in an EB (electrostatic and magnetic sector fields in series) geometry. An energy-selecting slit located between both sector fields can be closed to the extent that an energy resolution of $\Delta E/E\sim 10^{-3}$ is obtainable. With the secondary ions' pass energy of 4.5 keV,

this resolution translates into an energy bandpass of about 2–3 eV (see below). The Cs^+ primary-ion beam was produced in the instrument's Cs surface-ionization source. A focused (a few μm) 5.5-keV Cs^+ ion beam with a beam current in the range 0.2–1 nA was used here which was raster scanned, at an incidence angle of 42° relative to normal, across a sample area of $(125\ \mu\text{m})^2$. Secondary ions were accepted from a circular area of 60 μm in diameter centered within the bombarded region. Because of the high intensity of Cs^+ secondary ions, for this species the acceptance area was reduced to 8 μm to avoid detector saturation.

Energy distributions of secondary ions are measured by ramping the target potential around the 4.5-kV value, while keeping the remaining secondary-beam optics unchanged. Thus, with the energy slit closed, only ions within a narrow, constant total-energy range (the sum of the ion's kinetic emission energy plus the acceleration energy) can pass the slit and, subsequently, the magnetic sector. Changes of the surface WF are detected in this arrangement as a variation of the contact potential between the sample and the electrostatic analyzer; they result, therefore, in shifts of the secondary-ion energy distribution. Most accurately these shifts are determined from the steeply rising low-energy parts of the spectra. In order to register small WF variations, the sample-potential power supply was modified in a way that this potential could be varied in steps of 0.09 V. Checks have shown that the long-term stability (i.e., for the typical dwell time per step of ~ 1 s) is much better than that value. The total-energy width accessible under these conditions amounts to about 20 eV, which is completely sufficient for the present investigations. The working pressure of the instrument was about 1×10^{-9} mbar.

For the present experiments elemental samples of Al, Si, Nb, and Au were chosen, mostly because these elements cover a relatively wide range of sputtering yields,¹⁹ and are expected, therefore, to produce a varying degree of steady-state Cs surface concentration and possible work-function changes. The silicon sample was a (100) single crystal (*n* type, 5 Ω cm) which, however, is amorphized at fluences of $\sim 10^{14}$ cm^{-2} ,²⁰ well below the smallest fluence increment applied here. The Al, Nb, and Au specimens were polycrystalline films. The pristine surfaces of these elements also feature a certain range in work function: $\Phi_{\text{Si}}=4.85$ eV, $\Phi_{\text{Al}}=4.3$ eV, $\Phi_{\text{Nb}}=4.3$ eV, and $\Phi_{\text{Au}}=5.1$ eV.²¹

Computer simulations have been carried out using the T-DYN code²² to estimate the surface concentration of Cs as a function of the fluence. This program, based on the binary-collision approximation, simulates the dynamic evolution of collision cascades in solids evoked by an impinging projectile (Cs in the present case), thereby determining both the gradual incorporation of the bombarding ions and the possible composition changes of the target (e.g., in a multicomponent system).

RESULTS AND DISCUSSION

For Cs^+ ions sputtered from Si under Cs^+ impact, Fig. 1 shows energy distributions recorded at different bombarding fluences. To facilitate a comparison of the relevant features, they are depicted in a normalized way. A distinct shift of the spectra with increasing Cs^+ fluence is observed. Important, however, is the finding that the *complete* distributions are

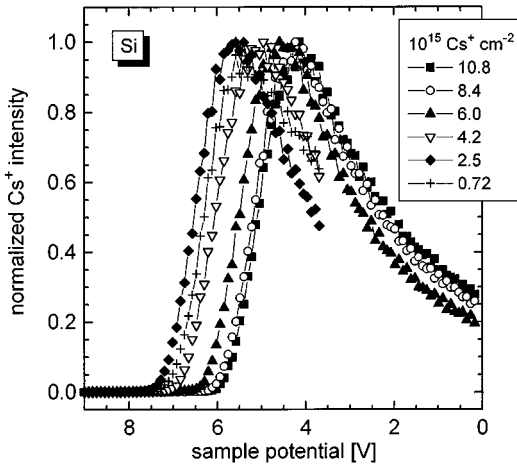


FIG. 1. Normalized energy spectra of Cs^+ sputtered from Si under 5.5-keV Cs^+ impact. The sample potential is given relative to the value of 4500 V, and the ions' emission energy increases from left to right in the plot. The parameter is the Cs^+ fluence.

shifted, and that the shape stays essentially unchanged. These shifts can therefore be ascribed to WF changes induced by the transient Cs incorporation. These relative changes are most easily derived from the low-energy portions of the spectra, but the peak positions also shift by an equal amount. The former were fitted with tangents, and intercepts of the latter with an energy scale were used, as done in electron spectroscopies,²³ to determine the relative changes of the work function induced by the gradual Cs buildup. This fitting is exemplified in Fig. 2(a), which shows, for SiCs^+ ions, the onset regions of the energy spectra; these SiCs^+ spectra also exhibit shifting related to WF changes.

The energy distributions of SiCs^+ depicted in Fig. 2(b) and the corresponding ones of Cs^+ show that the measured SiCs^+ and Cs^+ intensities increase initially with fluence, pass through a maximum, and decrease before reaching a stationary value. At fluences of about 10^{16} Cs^+/cm^2 , a saturation of the Cs concentration is reached, and the value of Φ levels off. The maximum shift then amounts to $\Delta\Phi \sim 1.3$ eV. These results are seen more clearly in Fig. 3, which depicts, as a function of Cs^+ fluence, the WF shift $\Delta\Phi$ and the intensities of Cs^+ and SiCs^+ ; the latter were extracted from the maxima of the respective energy distributions [cf. Figs. 1 and 2(b)]. The values of $\Delta\Phi$ were both evaluated from the Cs^+ and SiCs^+ data (normalized and absolute energy spectra yield the same values of $\Delta\Phi$ within the accuracy of the results), and are given relative to the largest value of Φ which, somewhat surprisingly, does not occur at the lowest fluence; at this latter fluence ($\sim 7 \times 10^{14}$ cm^{-2}) the work function is lower by about 0.3 eV (it is noted that a Cs^+ fluence of 1×10^{15} cm^{-2} corresponds to the removal of a layer of about 4 Å if the bulk sputtering yield of Si is assumed to be applicable). The reason for this observation is not clear, but might be related²⁴ to oxygen (or other impurity species) originally present on the surface when the Cs^+ bombardment was started.

This reduction of the WF (~ 1.3 eV) is clearly much smaller than that observed in Cs-adsorption experiments [about 3 eV (Ref. 25)]. The difference, very probably, is due to the lower Cs concentration in the present case and, per-

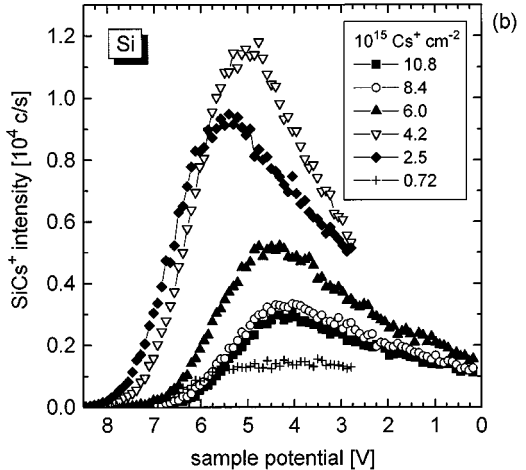
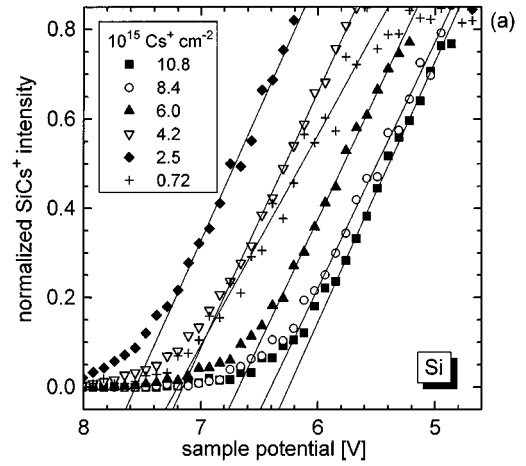


FIG. 2. (a) The onset regions of energy distributions of SiCs^+ ions sputtered from Si under 5.5-keV Cs^+ impact. The spectra are normalized to the maximum values and fitted with tangents to derive $\Delta\Phi$. The sample potential is given relative to the value of 4500 V, and the ions' emission energy increases from left to right in the plot. The parameter is the Cs^+ fluence. (b) The complete SiCs^+ energy spectra.

haps, a different site configuration of the Cs atoms (ions). While in Cs adsorption the Cs^+ ions sit on top of the substrate, this is not necessarily the case for the present implantation situation where Cs is replenished by implantation and concurrent sputter removal which exposes, at the surface, previously injected Cs atoms. It is by no means obvious whether these atoms (ions) are capable of forming a dipole layer to the same extent as do adsorbed ions. Notwithstanding these differences, even under dynamic conditions the WF changes drastically influence ions yields. The data show that, upon lowering the WF, the ion intensities start to deviate from the initially linear increase with fluence (the dashed line in the upper panel of Fig. 3) and, with a further reduction of Φ due to the still increasing Cs surface concentration, pass through a maximum and then saturate. Such a behavior (see also Ref. 26) must be ascribed to a *reduction* of the ionization probability for positive secondary ions (here Cs^+) with *decreasing* WF (a similar yield evolution with $\Delta\Phi$ has been reported for a static adsorption/desorption experiment²⁷). The finding that the SiCs^+ intensity closely follows that of Cs^+ , which supports the aforementioned formation process

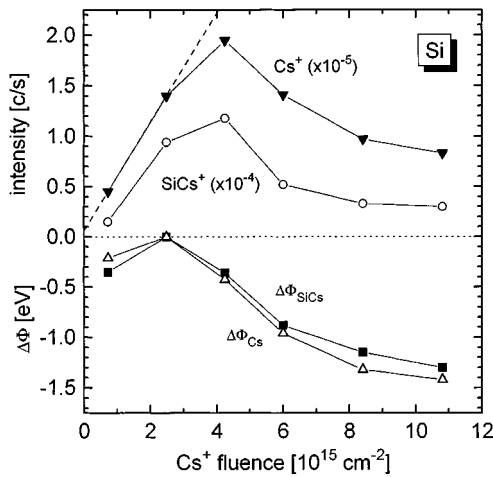


FIG. 3. The intensities of Cs⁺ and SiCs⁺ ions and the WF change $\Delta\Phi$ as a function of Cs⁺ fluence for a silicon sample. The dashed line in the upper panel indicates an expected linear increase of the Cs⁺ intensity with concentration.

of these MCs⁺ species (an association of a Si atom with a Cs ion), also appears rather important.

To obtain information on the Cs surface concentration during the gradual incorporation in the initial stage of irradiation, computer simulations were performed using the T-DYN code.²² This program dynamically determines the implantation and buildup of the bombarding species in the target. Figure 4(a) exemplifies this process by depicting, for different fluences, the Cs concentration as a function of depth in Si bombarded by 5.5-keV Cs. At low fluences the distribution is close to a standard implantation profile (roughly Gaussian, with a mean range of about 70 Å); with increasing fluence the distributions are found to approach a stationary state. Figure 4(b) shows the Cs surface concentration versus the Cs fluence derived from the implant distributions [Fig. 4(a) and others]. It is seen that the Cs surface concentration increases roughly in proportion to the implant fluence up to $\sim 1.5 \times 10^{16}$ Cs-atoms/cm², but saturates for a fluence of about 2×10^{16} Cs-atoms/cm². Then the Cs concentration amounts to ~ 12 at. %. Such a linear increase appears to agree with experiments^{4,28} studying, via ion backscattering spectroscopy, the Cs incorporation in Si, albeit at somewhat different bombarding energies and angles.

This linear increase of the Cs surface concentration obtained in the simulations has to be compared with the deviation from linearity of the Cs⁺ intensity (see Fig. 3) already at fluences of $> 2 \times 10^{15}$ cm⁻², i.e., at a value where the concentration is still increasing. Ascribing this deviation to a reduction of the Cs⁺ ionization probability, it is possible to determine P_{Cs^+} and to correlate it with the associated changes $\Delta\Phi$. Such data are shown in Fig. 5; they indicate that P_{Cs^+} is indeed constant (it is assumed here that $P_{Cs^+} = 1$) for small $\Delta\Phi$, but decreases drastically for $\Delta\Phi > 0.4$ eV, being a factor of 7 lower for the maximum WF change observed. From the measured Cs⁺ intensity at equilibrium (the partial Cs sputtering yield is unity then), the primary ion current, and the instrument transmission [$\sim 15\%$ (Ref. 18)], an experimental value of $P_{Cs^+} \sim 0.17$ is found which is in good agreement with the result depicted in Fig. 5 for Si. These data are in general agreement with results by Yu and

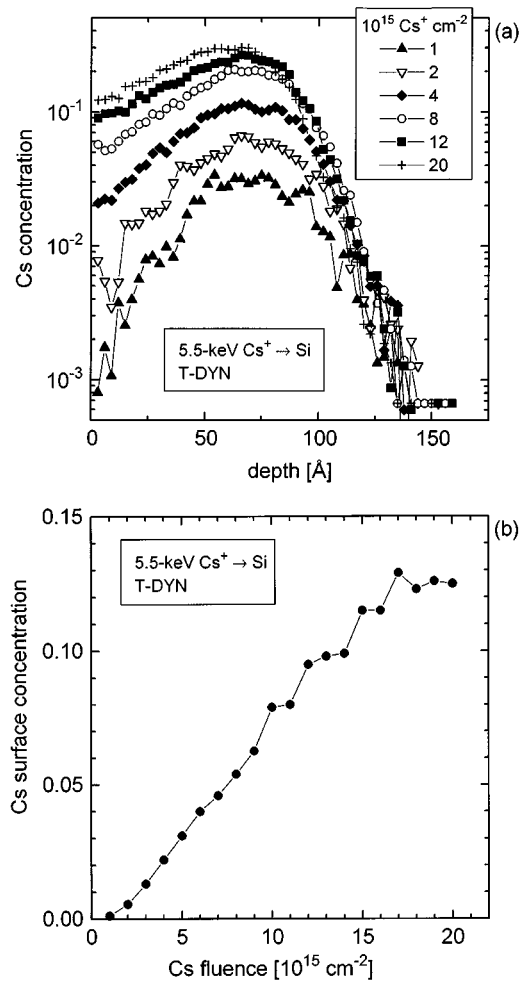


FIG. 4. Computer simulation data for 5.5-keV Cs impact on Si. (a) Cs concentration vs depth. The parameter is the Cs fluence. (b) Cs surface concentration as a function of Cs fluence.

Lang,⁷ who find a constant value of P_{Cs^+} for $\Phi > I$, and a pronounced reduction of Φ slightly below I_{Cs} . Contrary to those experiments, which determined an absolute scale for Φ , the present study can only derive relative changes of the WF. Nevertheless, a value $\Delta\Phi \sim 1$ eV, which corresponds to the factor-of-7 reduction of P_{Cs^+} (see Fig. 5), is close to what is reported by Yu and Lang.⁷

According to the simulations, a stationary Cs surface concentration is reached at a fluence of some 10^{16} Cs⁺/cm²; in the experiment, both $\Delta\Phi$ and the ion yields approach constant values at this fluence. The maximum WF shift (~ 1.3 eV) is less than that observed in adsorption studies^{24,25,29} which produce shifts of ~ 3 eV, albeit at considerably higher cesium coverages. Taking those investigations as a guideline, a value of $\Delta\Phi \sim 1.3$ eV would correspond to a Cs surface coverage of about 0.15 of a monolayer; the latter figure is close to the steady-state Cs concentration obtained from the computer simulations. This agreement should not be stressed too much, however, because of the above-discussed possible difference between static and dynamic conditions with regard to Cs occupation sites.

Apart from Si, ion emission under Cs⁺ irradiation was also studied in a similar manner for Al, Nb, and Au specimens. Figure 6 summarizes the implantation-fluence-

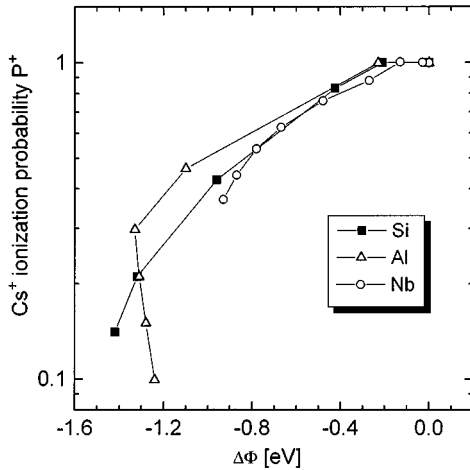


FIG. 5. The Cs^+ ionization probability P^+ vs work-function changes $\Delta\Phi$ for the Si, Al, and Nb specimens. Values of P^+ are derived through deviations of Cs^+ intensities from a linear increase with concentration (see Fig. 3 and text).

dependent changes of the WF and ion yields for an Al specimen bombarded by 5.5-keV Cs^+ ions. Similar to silicon, for the evaluation of $\Delta\Phi$ the shifts in the onset of the Cs^+ energy distributions were utilized. The WF is reduced to about 1.3 eV at a Cs^+ fluence of $\sim 4 \times 10^{15}$ ions/cm², and stays fairly constant for higher fluences. The Cs^+ and AlCs^+ intensities initially increase with Cs implantation; at the same fluence at which the lowering of the WF sets in, the Cs^+ yield starts to fall, while that of AlCs^+ continues to rise with increasing fluence. These signal evolutions of Cs^+ and AlCs^+ are clearly different from the respective ones observed for Si. One might suspect, however, that some emission of OCs^+ from the oxidized surface initially competes with and possible suppresses the formation of AlCs^+ . The deviation of the Cs^+ intensity from a linear increase can again be used to derive the variation of P_{Cs^+} (similar to Si, computer simulations also produce for Al a linear rise of the Cs surface concentration up to about 1×10^{16} cm⁻²; the saturation value is 10 at. %). These data are compiled in Fig. 5, and demonstrate a rapid decrease of P_{Cs^+} with the lowering of the WF, again in agreement with the data of Yu and Lang.⁷

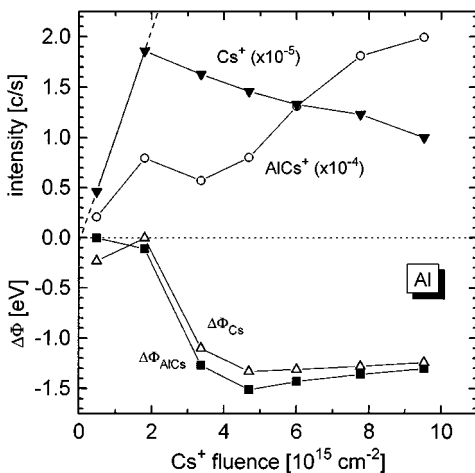


FIG. 6. As in Fig. 3, but for an Al specimen.

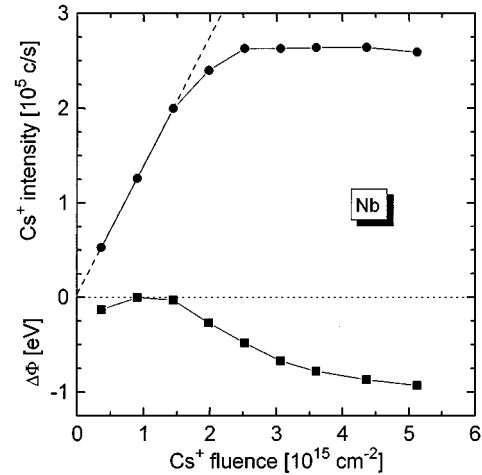


FIG. 7. As in Fig. 3, but for a Nb sample.

In the case of Nb, the experiments (Fig. 7) produce a linear increase of the Cs^+ yield up to a fluence of 1.5×10^{15} Cs^+/cm^2 ; beyond this value the intensity saturates, and the WF is reduced, reaching a maximum of $\Delta\Phi = -0.93$ eV. The corresponding computer simulations result in a linear increase of the Cs surface concentration up to about 5×10^{15} Cs^+/cm^2 , and a stationary value of 5.5 at. %. This lower concentration causes a smaller reduction of the work function as compared to Si and Al; it is probably due to the higher sputtering yield of Nb (about twice that of Si according to other experiments¹⁹ and the simulations). Employing the deviations of the Cs^+ intensity from linearity at low fluences (see the dashed line in Fig. 7) as a measure of the lowering of P_{Cs^+} , a strong decrease of P^+ is observed (Fig. 5) which starts at a modest $\Delta\Phi = -0.3$ eV. Since the WF of intrinsic Nb is 4.3 eV,²¹ this decrease coincides with $I_{\text{Cs}} \sim \Phi$. The experimentally derived ionization probability for Cs^+ sputtered under steady state from Nb amounts to $P_{\text{Cs}^+} \sim 0.39$, and comes close to the value shown in Fig. 5. The drastic reduction of P_{Cs^+} found for Al, Si, and Nb in the range $I_{\text{Cs}} \sim \Phi$ is in qualitative agreement with the electron-tunneling model of Yu and Lang,⁷ and the associated experiments of these authors. The present results appear to be a confirmation of this concept for *dynamic* Cs-incorporation conditions.

The results obtained for Au are distinctly different from those for Si and Al. Because of its higher sputtering yield [$Y_{\text{Au}} \sim 12$ atoms/ion, $Y_{\text{Si}} \sim 2.3$ atoms/ion Ref. 30], the equilibrium Cs concentration in Au should be correspondingly lower [under steady-state conditions, on average one Cs species is reemitted together with Y sample atoms; so the concentrations might scale like $1/(1+Y)$ to first order]. The T-DYN computer simulations produce a stationary Cs surface concentration of about 2.5%. This is also reflected in the experiments (here a sample potential of 3 keV was used to extend the spectrometer's mass range for the detection of AuCs^+ ; this results in a Cs^+ impact energy of 7 keV). A much smaller WF change was found ($\Delta\Phi = -0.4$ eV), reached already at a fluence of 4×10^{14} Cs^+/cm^2 , and a Cs^+ intensity which increases without passing through a maximum, see Fig. 8. Apparently, due to the small value of $\Delta\Phi$, the work function is not reduced below I_{Cs} (for the pristine

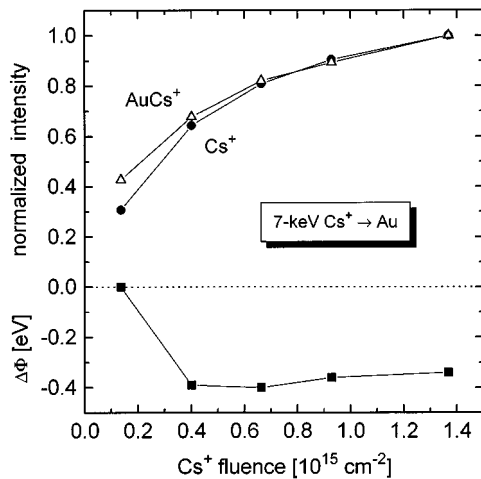


FIG. 8. As in Fig. 3, but for the Au sample. The Cs⁺ impact energy is 7 keV.

Au surface, $\Phi_{\text{Au}}=5.1$ eV); therefore, P_{Cs^+} is unity in the regime accessible for the present bombardment conditions. The Cs⁺ intensity in Fig. 8 thus directly reflects the buildup of the surface Cs concentration. Also, a close correlation between Cs⁺ and AuCs⁺ intensities during the Cs build-up is observed.

CONCLUSION

In summary, the present work investigated the possibility of determining work-function variations induced by Cs⁺ ion irradiation of surfaces. The onset of secondary-ion energy distributions can be used to monitor WF shifts *in situ* with a resolution of 0.1 eV. For Si, Al, Nb, and Au surfaces, Cs incorporation effects a lowering of the WF and, concurrently, a reduction of the ionization probability for positive Cs⁺ ions as soon as the WF becomes smaller than $\sim I_{\text{Cs}}$. This finding is in accordance with the electron-tunneling model of secondary-ion formation. The emission of MCs^+ generally exhibits a correlation with the Cs⁺ yield, although some deviations from a one-to-one scaling are observed. In future studies this correlation should be investigated in more detail, also monitoring, e.g., Cs₂⁺ ions. Furthermore, positively charged atomic ions of the substrate should be recorded in order to establish their yield dependence on the work function. The present method thus appears to provide access to the WF modifications occurring on solid surfaces during the gradual Cs⁺ incorporation, and their influence on sputtered ion emission.

ACKNOWLEDGMENT

The author is grateful to H. Oechsner for his support of this work.

- ¹V. E. Krohn, *J. Appl. Phys.* **33**, 3523 (1962).
- ²R. G. Wilson, F. A. Stevie, and C. W. Magee, *Secondary Ion Mass Spectrometry* (Wiley, New York, 1989).
- ³G. S. Tompa, W. E. Carr, and M. Seidl, *Surf. Sci.* **198**, 431 (1988).
- ⁴N. Menzel and K. Wittmaack, *Nucl. Instrum. Methods* **191**, 235 (1981).
- ⁵M. L. Yu, in *Sputtering by Particle Bombardment III*, edited by R. Behrisch and K. Wittmaack (Springer, Berlin, 1991), p. 91.
- ⁶J. E. Chelgren, W. Katz, V. R. Deline, C. A. Evans, R. J. Blattner, and P. Williams, *J. Vac. Sci. Technol.* **16**, 324 (1983).
- ⁷M. L. Yu and N. D. Lang, *Phys. Rev. Lett.* **50**, 127 (1983).
- ⁸H. Gnaser, *J. Vac. Sci. Technol. A* **12**, 452 (1994).
- ⁹M. L. Yu, *Phys. Rev. Lett.* **47**, 1325 (1981).
- ¹⁰M. J. Vasile, *Phys. Rev. B* **29**, 3785 (1984).
- ¹¹M. Bernheim and F. Le Bourse, *Nucl. Instrum. Methods Phys. Res. Sect. B* **27**, 94 (1987).
- ¹²K. Wittmaack, *Phys. Scr.* **T6**, 71, (1983).
- ¹³P. Sigmund, in *Sputtering by Particle Bombardment I*, edited by R. Behrisch (Springer, Berlin, 1981), p. 9.
- ¹⁴Z. Sroubek, *Nucl. Instrum. Methods* **194**, 533 (1982).
- ¹⁵A. P. Jansen, P. Akhter, C. J. Harland, and J. A. Venables, *Surf. Sci.* **93**, 453 (1980).
- ¹⁶G. Bachmann, J. Scholtes, and H. Oechsner, *Mikrochim. Acta* **I**, 489 (1989).
- ¹⁷G. Blaise and G. Slodzian, *Surf. Sci.* **40**, 708 (1973).
- ¹⁸H. N. Migeon, C. Le Pipec, and J. J. Le Goux, in *Secondary Ion Mass Spectrometry SIMS V*, edited by A. Benninghoven, R. J. Colton, D. S. Simons, and H. W. Werner (Springer, Berlin, 1986), p. 155.
- ¹⁹H. H. Andersen and H. L. Bay, in *Sputtering by Particle Bombardment I* (Ref. 13), p. 145.
- ²⁰W. Bock, H. Gnaser, and H. Oechsner, *Surf. Sci.* **282**, 333 (1993).
- ²¹H. B. Michaelson, *J. Appl. Phys.* **48**, 4729 (1977).
- ²²J. Biersack, S. Berg, and C. Nender, *Nucl. Instrum. Methods Phys. Res. Sect.* **59/60**, 21 (1991).
- ²³J. Scholtes, *Fres. J. Anal. Chem.* **353**, 499 (1995).
- ²⁴J. E. Ortega, E. M. Oellig, J. Ferron, and R. Miranda, *Phys. Rev. B* **36**, 6213 (1987).
- ²⁵R. E. Weber and W. T. Peria, *Surf. Sci.* **14**, 13 (1969).
- ²⁶K. Wittmaack, *Surf. Sci.* **126**, 573 (1983).
- ²⁷M. L. Yu, *Phys. Rev. B* **29**, 2311 (1984).
- ²⁸C. E. Christodoulides, W. A. Grant, and J. S. Williams, *Nucl. Instrum. Methods* **149**, 219 (1978).
- ²⁹C. A. Papageorgopoulos and M. Kamaratos, *Surf. Sci.* **221**, 263 (1989).
- ³⁰R. G. Wilson, S. W. Novak, S. P. Smith, S. D. Wilson, and J. C. Norberg, in *Secondary Ion Mass Spectrometry SIMS VI*, edited by A. Benninghoven, A. M. Huber, and H. W. Werner (Wiley, Chichester, 1988), p. 133.